International Journal of Computing and Digital Systems
ISSN (2210-142X)
Int. J. Com. Dig. Sys. #, No.# (Mon-20..)

Temperature Controlled Comfortable Chair with Light Therapy, and Features for Nyctophobia and Seasonal Affective Disorders

Vijay Mane[1], Harshal A. Durge[2]

[1,2,3] *Electronics and Telecommunication, Vishwakarma Institute of Technology, Pune, India*

vijay.mane@vit.edu, harshal.durge21@vit.edu

Received ## Mon. 20##, Revised ## Mon. 20##, Accepted ## Mon. 20##, Published ## Mon. 20##

Abstract: Prolonged sitting often results in discomfort, injury, and chronic pain, particularly for prehospital patients and manual wheelchair users who experience significant upper-limb pain and dysfunction. The Temperature Controlled Comfortable Chair (TCCC) addresses these issues by offering specialized relief and adaptable features. This study aims to develop a multifunctional chair to enhance comfort, mobility, and safety for individuals with varying medical needs. The TCCC integrates customizable sitting and sleeping arrangements, a temperature-regulated mattress, joystick-controlled mobility, and automatic lighting. Testing involved evaluating thermostat responses for heating and cooling functions and assessing the automatic lighting system under different light conditions. Results indicate that the TCCC effectively regulates temperature, maintaining comfort in varying weather conditions. The warming function facilitates drying, while the cooling function alleviates prickly heat. Automatic lighting activates in low-light scenarios, enhancing patient safety and addressing nyctophobia. The joystick-controlled mobility system, despite the chair's substantial weight, ensures effortless maneuverability. Data showed consistent performance of the automatic lighting feature across various light conditions, with specific lux levels triggering the DC light. The TCCC provides a comprehensive solution for prolonged sitting discomfort, integrating essential features to enhance user comfort and convenience. Its innovative design sets a new standard in ergonomic seating and sleeping solutions, suitable for both everyday and medical settings, emphasizing the importance of multifunctional and user-centric design in patient care.

Keywords: Detection, temperature, safety, mobility, illuminance

1. Introduction

Prehospital patients, particularly those with severe injuries or illnesses, are at a heightened risk of cold exposure, which can lead to hypothermia. Traditionally defined as a body core temperature below 35°C, hypothermia's definition has been revised to below 36°C due to its significant prognostic implications in trauma cases [1]. Hypothermia negatively impacts bodily functions, increasing morbidity and mortality regardless of injury severity [2]. Various factors, including fatigue, nervous system injuries, medication, alcohol, age, chronic illness, trauma, malnutrition, and endocrine disorders, disrupt the body's thermoregulatory mechanisms, leading to peripheral vasoconstriction and rapid cooling of the extremities and back [3].

Manual wheelchair users frequently encounter upper-limb pain and dysfunction, primarily due to propulsion and transfers, with up to 73% reporting chronic pain [4]. Biomechanical analyses of wheelchair propulsion have aimed to enhance mechanical efficiency and address musculoskeletal issues by investigating variables such as hand rim size, wheel camber, rim tube diameter, and seat position [5]. Despite these advances, 40% of electric wheelchair users still face maneuvering difficulties [6]. Recent research has integrated mobile robot guidance techniques into electric wheelchairs, yet challenges with joystick control persist due to physical limitations and spasticity-induced tremors [7].

Previous studies have explored the effects of seat position on wheelchair propulsion efficiency. Engel et al.

E-mail:vijay.mane@vit.edu, harshal.durge21@vit.edu

determined that positioning the seat unit posteriorly relative to the rear wheels was most efficient [8]. Brubaker's findings supported this by showing that a posterior seat placement reduces rolling resistance and enhances propulsion efficiency [9]. Van der Woude et al. identified that optimal elbow flexion angles significantly affect energy consumption and kinematics [10]. Hughes et al. established a robust correlation between seat position and joint motion during propulsion, emphasizing the need for ergonomically optimal seat positioning [11]. However, these studies often focus on static configurations and fail to address the dynamic needs of users.

This study aims to develop the Temperature Controlled Comfortable Chair (TCCC), a multifunctional seating solution that integrates customizable sitting and sleeping arrangements, temperature regulation, joystick-controlled mobility, and automatic lighting. The TCCC is designed to enhance comfort, mobility, and safety for individuals with varying medical needs, addressing the limitations of previous studies by offering a dynamic and adaptable solution tailored to individual user preferences and requirements. The TCCC represents a significant advancement in ergonomic design, setting a new standard for modern seating and sleeping solutions.

2. METHODOLOGY

This section presents detail of components connection illustrating the comprehensive features of the Temperature Controlled Comfortable Chair (TCCC), depicted in Fig. 1.

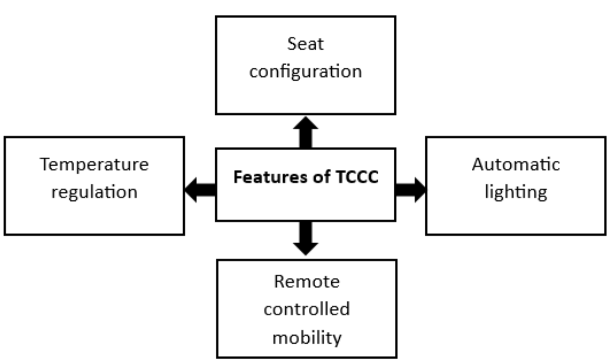

Figure 1 Features of TCCC

A. System overview

This section includes overview of 3 systems. First system is for automatic lighting and seat configuration, second system for seat temperature regulation, and third for remote controlled mobility.

The setup involves the integration of a diverse array of components to establish a sophisticated smart seating system. At its core, an Arduino Uno serves as the central control unit, interfacing with essential peripherals including a BH1750 light sensor, servo motor, potentiometer, and relay module. These components collectively enable automatic adjustments in lighting based on ambient conditions and user-defined seating configurations. Moreover, the TCCC incorporates dual thermostats tasked with managing a 12V DC fan and a 220V AC LED strip, pivotal for regulating seat temperatures through both warming and cooling functionalities. The chair's mobility is facilitated by an L298N motor driver module, BO motors, and a joystick interface, seamlessly integrated with the Arduino Uno. This integrated setup enables precise and remote-controlled adjustments, significantly enhancing user comfort and accessibility.

B. Hardware

The section presents the description of the following components used in system.

1) SG90 Servo motor

The SG90 servo motor is a compact, powerful motor capable of approximately 180-degree rotation. It operates within a closed-loop system that includes a motor, potentiometer, and control circuit as shown in Fig. 2. The gear system reduces speed and increases torque, while the potentiometer detects the shaft's position, converting it into an electrical signal for the control circuit. This circuit uses PWM signals for precise motor positioning. The embedded board interprets these signals, directing motor rotation and allowing continuous adjustments for accuracy and stability, ideal for precision applications [12][13].

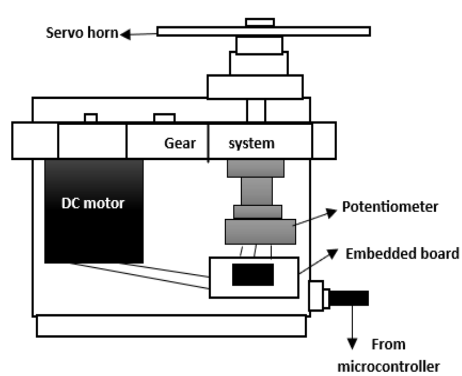

Figure 2 Servo motor module (internal structure)

2) 10K Potentiometer

A 10K potentiometer is used in this study to adjust the servo motor's angle by acting as an adjustable voltage divider. It regulates voltage and adjusts resistance within electronic circuits. The potentiometer has three terminals: two fixedend terminals and a sliding contact (wiper). Internally, it provides variable resistance; terminals 1 and 3 have a fixed 10kΩ resistance, with the wiper adjusting between them. At the midpoint, terminals 1-2 and 2-3 each measure 5kΩ, enabling precise resistance adjustment with the potentiometer knob. This adjustment follows Ohm's law, where varying the wiper position alters the voltage divider ratio, thus controlling the servo motor's angle effectively [14][15].

3) BH1750 light sensor

The BH1750 light sensor, utilizing an IC with an I2C interface, measures ambient light up to 65535 LUX, operating between 2.4V and 3.6V. A photodiode converts light into electrical signals with low current consumption. The sensor includes a voltage regulator and 4.7kΩ pull-up resistors on the SDA and SCL pins. Internally, it processes the photodiode's current signal via an operational amplifier, converting it to voltage, which an ADC digitizes to measure illuminance in LUX. The sensor's logic and I2C interface handle conversion and communication, with a 320kHz internal oscillator providing timing [16][17].

4) 5V Relay module

The 5V relay module, controlled by a microcontroller, acts as an electromagnetic switch. When triggered by a low-power signal, an electromagnet within the module is energized, moving an internal switch between Normally Closed (NC) and Normally Open (NO) positions. Initially, the Common (COM) terminal is connected to the NC terminal. When activated, the electromagnet switches the COM terminal to the NO terminal. Upon deactivation, it returns to its default state, reconnecting COM to NC and reopening NO, thus deactivating the relay [18][19].

5) Dual axis joystick

The joystick module enables directional input for chair movement via a microcontroller, using integrated potentiometers for X and Y-axis movements. It features a self-centering spring and a momentary pushbutton switch. At rest, it outputs 2.5V on both axes, translating stick positions into electrical signals. The module includes two 5kΩ potentiometers arranged orthogonally for precise movement detection. These potentiometers act as adjustable voltage dividers, providing analog outputs proportional to the joystick's position. The pushbutton switch toggles between digital HIGH and LOW states. Rotating the joystick knob adjusts the potentiometers, changing resistance and voltage outputs (0 to 1023), ensuring precise control and measurement based on joystick positioning [20][21].

6) L298N motor driver module

The mobility system uses the L298N dual H-Bridge motor driver to control four brushed DC motors, managing both direction and speed. It supports voltages from 5V to 35V and currents up to 2A, suitable for DC motors and compliant with TTL logic levels. The L298N includes two full-bridge power stages (A and B) in a bridge configuration, with external resistors for current sensing. Input signals (In1, In2, EnA for Bridge A; In3, In4, EnB for Bridge B) control motor direction and operation. The H-bridge setup manipulates input voltage polarity through four switches for direction control [22][23].

7) BO motors

Battery-operated (BO) motors provide efficient, low-power operation within durable plastic or metal casings. They feature a shaft for connecting to wheels or gears. Internally, they have a rotor with coil windings around an armature, surrounded by a stator with permanent magnets. When current flows through the rotor coils, electromagnetic interaction with the stator's field causes rotation. A segmented copper commutator reverses the current in the coils to sustain rotation, while carbon brushes maintain contact with the commutator, ensuring efficient conversion of electrical energy to mechanical motion [24].

8) Arduino Uno

The Arduino Uno, based on the ATmega328P, is a popular microcontroller board used in embedded systems and DIY electronics projects. It is renowned for its ease of use, versatility, and strong community support, making it suitable for beginners and advanced users. Key specs include a 5V operating voltage, 7-12V input range, 14 digital I/O pins (6 with PWM), 6 analog inputs, and a DC current of 20 mA per I/O pin. It features 32 KB flash memory (0.5 KB for the bootloader), 2 KB SRAM, 1 KB EEPROM, and a 16 MHz clock speed. The Arduino IDE simplifies programming for various projects [25][26][27].

9) XH W3001 Digital Thermostat

The XH-W3001 temperature controller is a digital device for precise temperature regulation, featuring programmable settings and a relay for controlling external devices. It operates on 220V AC or 12V DC and uses a 10k NTC thermistor to monitor temperatures from -50°C to 100°C with +/-0.1°C accuracy. Users can set heating thresholds by adjusting start and stop temperatures via simple button commands. To activate heating mode, set the min temperature by holding the down arrow for 3 seconds and adjusting, then set the max temperature by holding the up arrow for 3 seconds and adjusting. The stop temperature must be higher than the start temperature for heating mode; otherwise, it defaults to cooling mode [28][29].

10) 220V AC LED strip

A 220V AC LED strip with plastic coating operates directly on 220V AC mains without a transformer or driver. The plastic coating provides insulation and protection, making it suitable for both indoor and outdoor use. These strips are easy to install, can be cut to custom lengths, and offer efficient, bright lighting. Heat is generated mainly through the inefficiencies in the LED chips and associated electronics, as well as resistors used for current regulation, which also dissipate energy as heat [30].

11) 12V DC cooling fan

A 12V DC cooling fan is essential for heat dissipation in electronic and mechanical systems. It runs on a 12V DC power supply and is commonly used in computer cases and power supplies. The fan features a rotor with blades, a stator with windings, and a commutation circuit. When powered, current flows through the stator, creating a magnetic field that interacts with the rotor's permanent magnets, causing the rotor to spin and move air through the blades for effective cooling [31].

3. WORKING

This section outlines the operational flow of each feature of the TCCC and documents the results obtained during testing.

A. Seat configuration

Seat configuration feature leverages three servo motors to adjust the chair into various configurations for sitting or sleeping, providing ergonomic relief and addressing diverse user needs. A potentiometer is used to precisely control the servo motors, enabling smooth transitions between positions. The system supports multiple configurations, each tailored to a specific function. The eleven distinct chair positions, delineated in Table I and depicted in Fig. 3, serve specific functions crucial for health recovery. The table II presents various chair configurations and their respective purposes, determined by specific servo motor angles (θ1, θ2, θ3).

1.

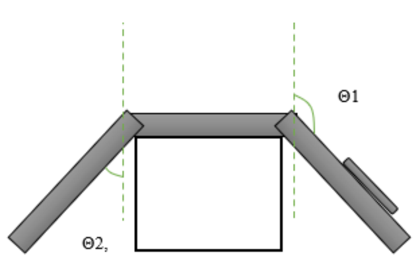

2.

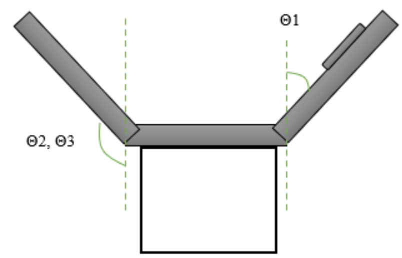

3.

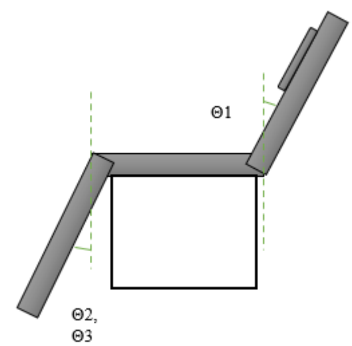

4.

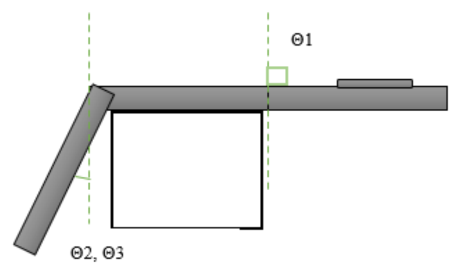

5.

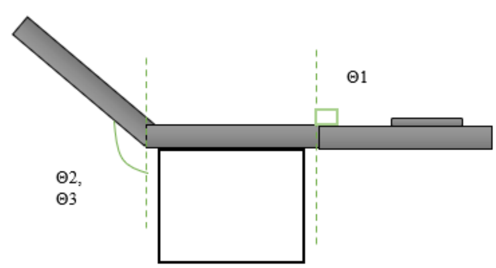

6.

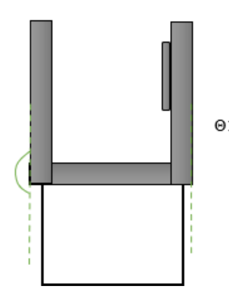

7. 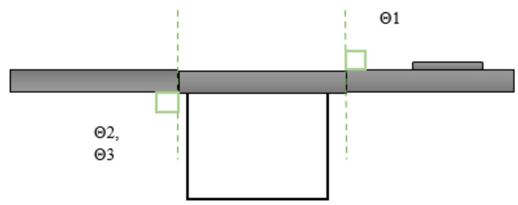

8. 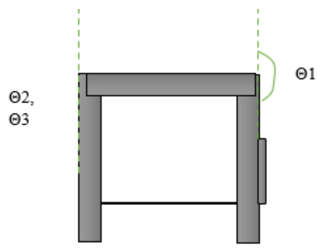

9. 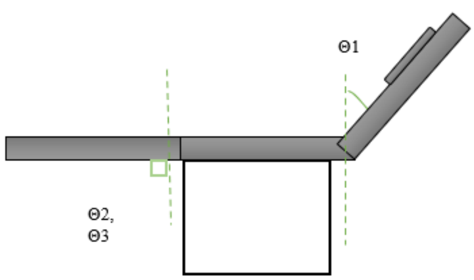

10. 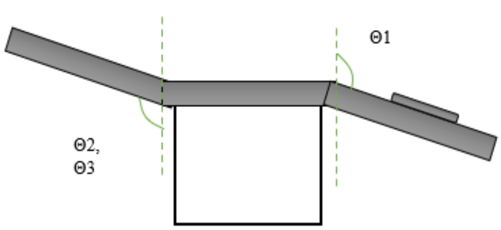

11. 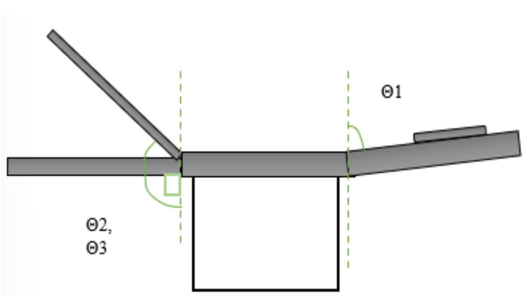

Figure 3 Seat configurations

These positions incorporate features such as abdominal exercise facilitation, relaxation promotion, and support during recovery from injury or surgery. They are designed to address various health needs, including muscle strengthening, weight loss, stress reduction, and circulatory improvement. Additionally, the configurations offer customizable seating and sleeping options, optimizing comfort, posture, and therapeutic benefits. Notably, the positions cater to diverse requirements such as leg elevation for enhanced circulation, back support for spinal alignment, and reclined postures for tension relief. Specific designs accommodate rehabilitation needs, such as aligning leg fractures and minimizing discomfort during rest and sleep.

The user adjusts the potentiometer's knob to specific angles indicated by an arrow, altering the resistance of the wiper and varying the voltage according to Equation (1).

$$V_{out} = V_{in} * \frac{R_{wiper}}{R_{total}} \quad (1)$$

where R_{total}=10k ohm
This analog voltage is converted into a digital value by the Arduino Uno's 10-bit ADC using Equation (2).

$$ADC_{value} = \frac{V_{out}}{V_{in}} * 1023 \quad (2)$$

where V_{in}=5V
The digital value is then applied to Equation (3) to determine the corresponding servo angle, setting the servo motor's position accurately.

$$Angle = \frac{ADC_{value}}{1023} * 180 \quad (3)$$

The obtained data is documented in Table I, which shows the corresponding wiper resistance values for specific servo angles.

TABLE I CORRESPONDENCE BETWEEN SERVO ANGLES AND WIPER RESISTANCE VALUES

Servo angle	Wiper resistance value (ohm)
0˚	0
30˚	1.67k
45˚	2.5k
75˚	4.17k
90˚	5k
120˚	6.67k
135˚	7.5k
180˚	10k

In the control section of the chair, three potentiometers are installed, each labeled with specific angles as illustrated in Fig. 4. As the arrow indicates a particular angle, the servo motor adjusts accordingly to align with the corresponding angle.

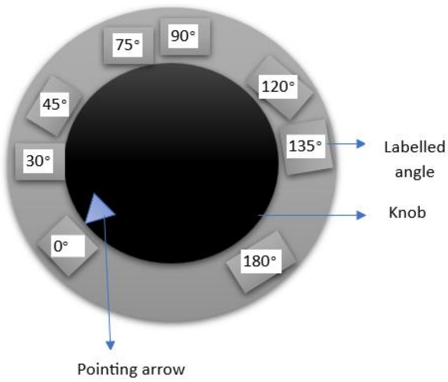

Figure 4 Potentiometer with labelled angles

The XH-W3001 220V AC thermostat is the central device for temperature control, incorporating an integrated relay to manage an LED strip's operation. Operating on a 220V AC power source, the module uses an embedded temperature sensor to monitor the current temperature and compare it to a predefined set point. Based on this comparison, the relay activates or deactivates to control the LED strip, which serves as a heat source by converting electrical energy into warmth through its resistive material composition.

During winter and rainy seasons, the thermostat module maintains optimal comfort levels by initiating the heating process. If the ambient temperature falls below the set threshold of 25°C, the relay activates, causing the LED strip to emit heat. This heat permeates the chair's foam material, raising its temperature. Once the temperature reaches or exceeds 25°C, the relay deactivates, allowing the temperature to drop until it reaches 20°C. The relay then reactivates to resume the heating cycle, ensuring consistent comfort.

Conversely, during the summer season, the thermostat module operates in cooling mode to alleviate heat discomfort. When the ambient temperature exceeds 25°C, the relay activates, powering a DC cooling fan to generate a stream of cold air. This airflow cools the foam, reducing its temperature. When the temperature drops to or below

TABLE II SEAT CONFIGURATION AND PURPOSE

Configuration number	Configuration name	Angle (ϴ1, ϴ2, ϴ3)	Purpose
1	Abdominal Exercise and Weight Loss	135°, 45°, 45°	Abdominal exercise and weight loss
2	Hammock-type configuration	45°,135°, 135°	relaxation, reducing stress levels
3,4	Sitting Chairs with Adjustable Seating	30°, 30°, 30° 90°, 30°, 30°	optimal comfort and support, recovering from injury or surgery
5,6	Sleeping Positions with Leg Elevation, side supported stool type configuration	90°, 120°, 120° 0°, 180°, 180°	improve circulation, reduce swelling, and alleviate pressure on the lower back and joints and comfortable rest while minimizing strain on the spine
7	Standard Bed Configuration	90°, 90°, 90°	restful sleep and overnight recovery, supporting immune function, cognitive function, and physical recovery
8,9	Stool-type configuration, and Semi-Sleeper Seats	180°, 0°, 0° 30°, 90°, 90°	sit comfortably without putting undue pressure on the spine or lower back, relieve tension, and promote relaxation
10	Lazy Sleeping Position	120°, 120°, 120°	maintaining body balance and reducing strain on muscles and joints
11	Leg Fracture Recovery Position	75°, 90°, 135°	recovering from leg fractures, adjusting the leg portion of the seat facilitates proper alignment and support

B. Seat temperature regulation

The Temperature Controlled Comfortable Chair features a sophisticated system designed to adapt to seasonal temperature variations, utilizing two XH-W3001 thermostat modules with separate power supplies to regulate seat temperature for winter, rainy, and summer conditions.

20°C, the relay deactivates, allowing the temperature to rise until it reaches 25°C. The relay then reactivates to sustain the cooling process, maintaining a comfortable seating temperature.

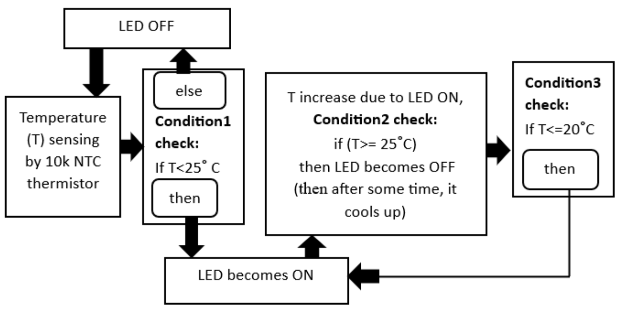

Figure 5 Warming system working

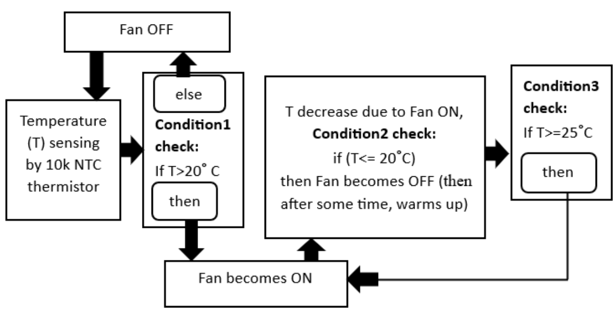

Figure 6 Cooling system working

This cyclic process continues until the power supply to the module is terminated, ensuring continuous temperature regulation adapted to seasonal conditions. Detailed operational diagrams are provided in Fig. 5 and 6, illustrating the complete functionality of the warming and cooling features, respectively.

C. Remote control mobility

This feature controls the mobility of the chair using a joystick.

The joystick provides analog input signals representing movement along the X and Y axes, which are transmitted to the microcontroller. These analog signals are converted to digital data using the Arduino Uno's 10-bit ADC, as described by Equation 4:

$$Digital_{value} = \left(\frac{Analog\_voltage}{V_{ref}}\right) * 1023 \tag{4}$$

Upon receiving the joystick input, the microcontroller interprets the digital data to determine the joystick's precise position. This positional information is used to activate the motor driver module. The L298N motor driver, incorporating an H-Bridge circuit, manages the current flow to the BO motors, dictating the chair's movement in response to joystick manipulation. Forward or backward movement along the Y-axis corresponds to forward or backward chair motion, while movement along the X-axis dictates side-to-side motion.

The H-Bridge circuit regulates motor rotation direction by selectively enabling or disabling switches based on the desired movement. When all switches (Out1, Out2, Out3, and Out4) are open, no current flows, resulting in a motor halt. For forward motion, switches Out1 and Out3 are set to HIGH, while Out2 and Out4 remain LOW. For reverse movement, Out1 and Out3 are LOW, and Out2 and Out4 are HIGH. For leftward motion, Out1, Out2, and Out4 are LOW, and Out3 is HIGH. Conversely, for rightward motion, Out2, Out3, and Out4 are LOW, and Out1 is HIGH.

$$output = (input - in_{min}) * \left(\frac{out_{max} - out_{min}}{in_{max} - in_{min}}\right) + out_{min} \tag{5}$$

Where:

- input = Y-axis joystick value
- in_min = Minimum Y-axis joystick value (0)
- in_max = Maximum Y-axis joystick value (1023)
- out_min = Minimum motor speed (-255 for backward)
- out_max = Maximum motor speed (255 for forward)

The microcontroller maps the digital values of the X and Y axes to determine the direction and speed of the motors. If the X-axis digital value is less than 512, it signifies left direction; if greater than or equal to 512, it signifies right direction. For the Y-axis, a value of 0 indicates backward movement, while 1023 indicates forward movement.

Motor speed is adjusted based on the mapped direction and the Y-axis digital value derived from Equation 5. Positive values for the left motor speed denote forward movement, while negative values indicate backward movement. The same logic applies to the right motor speed.

This precise control mechanism, illustrated in Fig. 7, ensures smooth and accurate chair movement in designated directions. Table III documents the observed data during testing, correlating joystick directions with the corresponding chair movements, provides a comprehensive overview of how joystick inputs translate into motor control signals, enabling nine directional movements, with analog values converted to digital bits by the microcontroller.

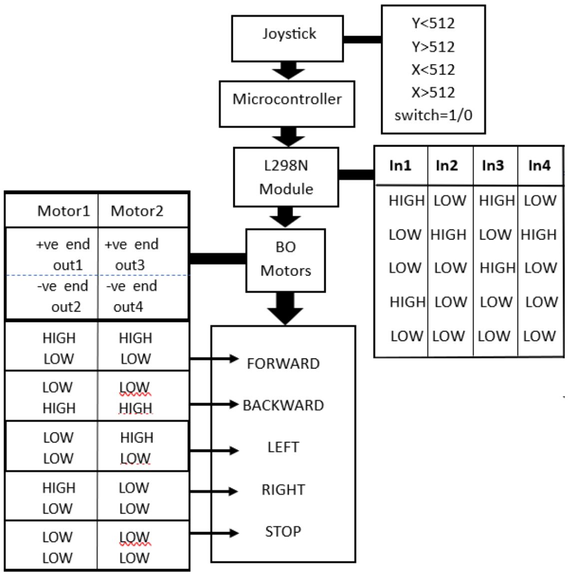

Figure 7 Working of remote controlled mobility system

The built-in Analog-to-Digital Converter (ADC) then transforms this voltage into 16-bit digital data representing luminance in Lux. The sensor's internal logic unit processes and outputs the digital Lux data via I2C communication, with a 320kHz internal clock oscillator providing the timing reference. If the measured lux value is below 300, the relay module's Common (COM) terminal connects to the Normally Open (NO) terminal, activating a DC LED. Conversely, if the lux value exceeds 300, the COM terminal connects to the Normally Closed (NC) terminal, turning off the DC LED. This mechanism enables automated lighting adjustments based on ambient brightness, ensuring optimal illumination for user comfort and convenience.

TABLE III JOYSTICK DIRECTIONAL INPUTS AND CORRESPONDING MOTOR CONTROL SIGNALS

Joystick direction	**Analog value (X, Y) in volts**	**Digital value (X, Y)**	**Mapped X axis (direction)**	**Mapped Y axis (motor direction)**	**Left motor speed**	**Right motor speed**	**Vehicle moving direction**
Center	(2.5V, 2.5V)	(512, 512)	-	0	0	0	stop
Full left	(0V, 2.5V)	(0, 512)	Left	-	-200	200	Left
Full right	(5V, 2.5V)	(1023, 512)	Right	-	200	-200	Right
Full up	(2.5V, 0V)	(512, 0)	-	-255	-255	-255	Backward
Full down	(2.5V, 5V)	(512, 1023)	-	255	255	255	Forward
Up left	(0V, 0V)	(0, 0)	Left	-255	-255	-200	Backward-left
Upright	(5V, 0V)	(1023, 0)	Right	-255	-200	-255	Backward-right
Down left	(0V, 5V)	(0, 1023)	Left	255	200	255	Forward-left
Downright	(5V, 5V)	(1023, 1023)	Right	255	255	200	Forward-right

D. Automatic lighting

In this, the BH1750 light intensity sensor is employed to measure ambient luminosity. As sensor's photodiode detects incident light, creating electron-hole pairs within the PN junction through the internal photoelectric effect. This generates an electrical signal proportional to the light intensity, which is subsequently converted into voltage by an integrated operational amplifier (OP-AMP). Working procedure is mentioned in Fig. 8.

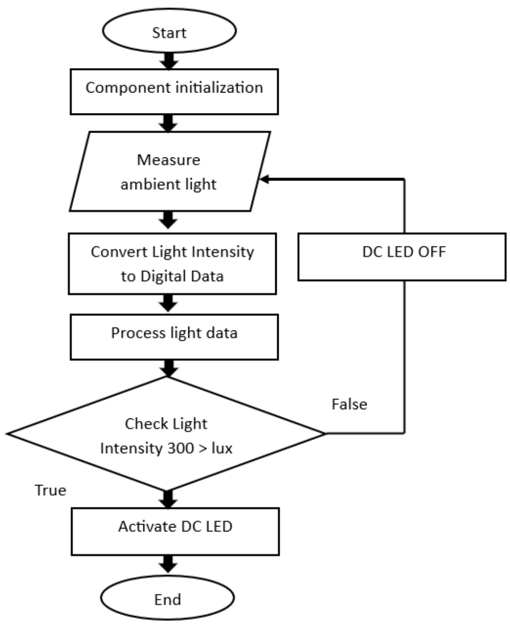

Figure 8. Workflow of Automatic lighting

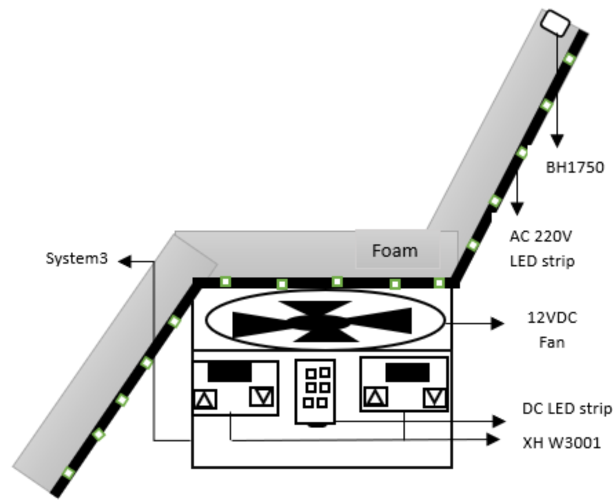

Figure 9 Placement of temperature regulation components on TCCC

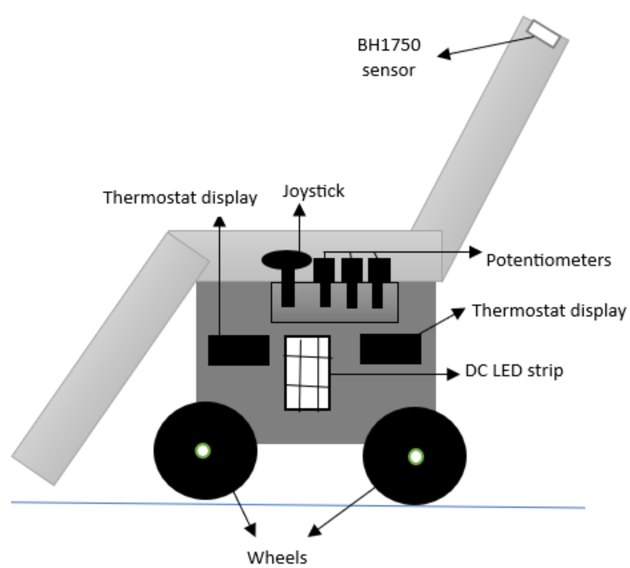

Figure 10 Placement of Automatic lighting and seat configuration modules on TCCC (outer appearance)

4. ARCHITECTURE

This section provides an architectural overview of the Temperature Controlled Comfortable Chair (TCCC), highlighting the integration of various system components as depicted in Fig. 9, 10. Fig. 9 illustrates "System3," which encompasses the warming and cooling system. Positioned beneath the seat, the 220V AC LED strip provides warmth to the foam, while a DC cooling fan directs airflow upwards from a ventilated box. Two thermostats regulate this system, ensuring optimal temperature control. An external DC LED strip on the box's surface ensures uniform illumination. The BH1750 light sensor, crucial for ambient light detection, is mounted atop the chair. In Fig. 10, "System1" includes the servo motor control system, potentiometers, automatic lighting with a relay module, BH1750 sensor, and external DC LED strip. Potentiometers are placed near the hand position, facilitating user control, while the light sensor and LED strip are strategically positioned for efficient operation.

5. RESULT

This section presents findings from testing Automatic Lighting and temperature regulation features as detailed in Tables IV and V.

Table IV evaluated lighting conditions with a set threshold of 300 lux, where the DC LED was deactivated when ambient light exceeded this level. In low-light environments like very dark settings (55 lux) and indoor dim conditions (258 lux), the LED provided necessary illumination. Conversely, at higher indoor light levels (392 lux), the LED automatically switched off to conserve energy. Outdoors under dim light (5076 lux) and on cloudy days (10601 lux), the LED remained off, effectively utilizing natural light.

TABLE IV LIGHT INTENSITY AND LED STATUS

Environmental condition	Measured lux values	DC LED status
Very Dark	55	ON
Dim (at home)	258	ON
Dim (at home)	392	OFF
Dim (below open sky)	5076	OFF
Cloudy (below open sky)	10601	OFF

This responsive strategy optimizes energy consumption by activating the LED only when necessary, ensuring sufficient lighting while supporting sustainable energy practices and addressing concerns such as Nyctophobia.

The temperature regulation feature was tested with minimum and maximum thresholds set at 20°C and 25°C for warming, and 25°C and 20°C for cooling, respectively. Table V illustrates the system's adaptive response to varying seasonal and daily temperatures, aiming to maintain optimal indoor comfort while minimizing energy usage. During hot summer periods, both during the day and night, the cooling system activated when temperatures exceeded 25°C, effectively managing indoor heat levels. For instance, at 37.2°C, the cooling system engaged, with continued operation at 41.5°C and 41.7°C to maintain comfort. At night, temperatures such as 29.1°C and 28.8°C remained above the cooling threshold of 25°C, necessitating the system's continuous operation.

In the rainy season, the warming system activated as temperatures fell below 20°C. During daytime temperatures around 21.9°C and 22.2°C, the warming system remained off since these temperatures exceeded the minimum threshold. However, at night, temperatures dropping to 19.1°C, 18.9°C, and 18.7°C activated the warming system to maintain indoor warmth. During winter days, temperatures at 25.3°C and 25.6°C exceeded the maximum warming threshold of 25°C, resulting in the deactivation of the warming system. Conversely, nighttime temperatures of 16.6°C, 16.1°C, and 15.9°C fell below the minimum threshold of 20°C, necessitating the warming system's activation to ensure comfort.

These results underscore the system's efficiency in maintaining precise climate control through adaptive responses to environmental conditions, thereby optimizing energy utilization and enhancing indoor comfort effectively.

TABLE V SEASONAL TEMPERATURE CONTROL STATUS

Season	Day/Night	Measured temperature	Cooling status	Warming status
Summer	Day	37.2	ON	Deactivated
	Day	41.5	ON	
	Day	41.7	ON	
	Night	28.8	ON	
	Night	29.1	ON	
Rainy	Day	22.2	Deactivated	ON
	Day	21.9		ON
	Night	18.9		ON
	Night	18.7		ON
	Night	19.1		ON
Winter	Day	25.6	Deactivated	OFF
	Day	25.3		OFF
	Night	16.6		ON
	Night	16.1		ON
	Night	15.9		ON

DISCUSSION

This study highlights the Temperature Controlled Comfortable Chair (TCCC) as a significant advancement in user comfort, integrating advanced lighting and temperature regulation. The automatic lighting system, set at a 300 lux threshold, activates LED illumination in low light and turns it off when ambient light is sufficient, optimizing energy use and aiding users with nyctophobia. The temperature control system effectively adapts to environmental changes, using thresholds of 20°C for warming and 25°C for cooling to maintain comfort. During hot weather, the cooling system activates above 25°C, while the warming system engages below 20°C during cooler periods. This adaptability ensures a comfortable environment year-round.

The TCCC's multifunctional design represents a major leap from traditional systems that focus solely on biomechanical efficiency, offering real-time adjustments to meet diverse user needs. Unlike previous studies that concentrated on wheelchair propulsion and seat positioning, the TCCC addresses dynamic environmental comfort. However, the study's controlled testing environment may not fully reflect real-world conditions, and the system's weight and mobility could be challenging for users with severe physical limitations. Future research should focus on field testing, improving sensor reliability, and exploring additional features to enhance user experience and adaptability.

CONCLUSION

This study aimed to develop the Temperature Controlled Comfortable Chair (TCCC), a multifunctional seating solution designed to improve comfort, mobility, and safety for individuals with diverse medical needs. The TCCC features customizable sitting and sleeping arrangements, temperature regulation, joystick-controlled mobility, and automatic lighting, targeting discomfort and pain from prolonged sitting, particularly for prehospital patients and manual wheelchair users. Results showed the TCCC's effectiveness in managing lighting and temperature. The lighting system, set at a 300 lux threshold, optimized energy use while ensuring adequate illumination in low-light conditions. The temperature regulation system adjusted to various environmental conditions, with cooling activated above 25°C and warming below 20°C, maintaining a comfortable indoor climate.

Despite these promising outcomes, further research is needed to address limitations. Future studies should include extensive field testing in diverse conditions to validate performance in real-world scenarios, including extreme weather and fluctuating power supplies. Improving sensor reliability and addressing potential technical issues are crucial. Additionally, optimizing the TCCC's weight and mobility for users with severe physical limitations and confined spaces, as well as expanding features for enhanced adaptability, will further improve user experience and effectiveness.

REFERENCES

[1] L. M. Aitken, J. K. Hendrikz, J. M. Dulhunty, and M. J. Rudd, "Hypothermia and associated outcomes in seriously injured trauma patients in a predominantly sub-tropical climate," Resuscitation, vol. 80, no. 2, pp. 217-223, Feb. 2009.

[2] V. Hultzer, X. Xu, C. Marrao, G. Bristow, A. Chochinov, and G. G. Giesbrecht, "Pre-hospital torso-warming modalities for severe hypothermia: a comparative study using a human model," CJEM, vol. 7, no. 6, pp. 378, Nov. 2005.

[3] J. LeBlanc, M. B. Ducharme, L. Pasto, and M. Thompson, "Response to thermal stress and personality," Physiol. Behav., vol. 80, no. 1, pp. 69-74, Oct. 2003.

[4] N. S. Lintu, M. A. Mattila, J. A. Holopainen, M. Koivunen, and O. O. Hänninen, "Reactions to cold exposure emphasize the need for weather protection in prehospital care: an experimental study," Prehosp. Disaster Med., vol. 21, no. 5, pp. 316-320, Oct. 2006.

[5] J. V. Subbarao, J. Klopfstein, and R. Turpin, "Prevalence and impact of wrist and shoulder pain in patients with spinal cord injury," J. Spinal Cord Med., vol. 18, no. 1, pp. 9-13, Jan. 1995.

[6] S. Guo, R. A. Cooper, M. L. Boninger, A. Kwarciak, and B. Ammer, "Development of power wheelchair chin-operated force-sensing joystick," in Proc. Second Joint 24th Annu. Conf. and the Annu. Fall Meeting of the Biomed. Eng. Soc., Eng. Med. Biol., vol. 3, pp. 2373-2374, Oct. 2002.

[7] D. Ding, R. A. Cooper, and D. Spaeth, "Optimized joystick controller," in Proc. 26th Annu. Int. Conf. IEEE Eng. Med. Biol. Soc., vol. 2, pp. 4881-4883, Sep. 2004.

[8] P. Engel, M. Neikes, K. Bennedik, G. Hildebrandt, and F. W. Rode, "Work physiological studies performed to optimate the lever propulsion and the seat position of a lever propelled wheelchair (author's transl)," Die Rehabilitation, vol. 15, no. 4, pp. 217-228, Nov. 1976.

[9] C. E. Brubaker, "Wheelchair prescription: an analysis of factors that affect mobility and performance," J. Rehabil. Res. Dev., vol. 23, no. 4, pp. 19-26, Oct. 1986.

[10] L. H. Van der Woude, D. J. Veeger, R. H. Rozendal, and T. J. Sargeant, "Seat height in handrim wheelchair propulsion," J. Rehabil. Res. Dev., vol. 26, no. 4, pp. 31-50, Jan. 1989.

[11] C. J. Hughes, W. H. Weimar, P. N. Sheth, and C. E. Brubaker, "Biomechanics of wheelchair propulsion as a function of seat position and user-to-chair interface," Arch. Phys. Med. Rehabil., vol. 73, no. 3, pp. 263-269, Mar. 1992.

[12] A. M. Haidar, C. Benachaiba, and M. Zahir, "Software interfacing of servo motor with microcontroller," Unpublished report.

[13] A. S. Sadun, J. Jalani, J. A. Sukor, and B. Pahat, "A comparative study on the position control method of dc servo motor with position feedback by using arduino," in Proc. Eng. Technol. Int. Conf., ETIC, pp. 10-11, Aug. 2015.

[14] I. Amri, E. D. Atmajati, R. A. Salam, E. Yuliza, and M. M. Munir, "Potentiometer a simple light dependent resistor-based digital," in Proc. 2016 Int. Semin. Sensors, Instrum., Meas., Metrol., ISSIMM, pp. 24-27, Aug. 2016.

[15] H. B. Brooks, "A new potentiometer for the measurement of electromotive force and current," U.S. Government Printing Office, 1906.

[16] A. Hachmi, M. El Hadi, R. Essaadaoui, O. Mommadi, A. Ouariach, and A. El Moussaouy, "Development of an educational device, based on Arduino, to facilitate the understanding of light diffraction," Phys. Educ., vol. 57, no. 4, pp. 045032, May 2022.

[17] X. He, Z. Xiao, and S. He, "A design of LED adaptive dimming lighting system based on incremental PID controller," in LED Display Technol., vol. 7852, pp. 164-170, Nov. 2010.

[18] V. Gurevich, Electric relays: principles and applications, CRC Press, Oct. 2018.

[19] R. R. Eniliev, "Principle of operation and application area of electromagnetic relay," in Proc. АНГЛИЙСКИЙ ЯЗЫК В СФЕРЕ ПРОФЕССИОНАЛЬНОЙ КОММУНИКАЦИИ, pp. 59-60, 2019.

[20] H. Kato and M. Kurisu, "Representation of the joystick using the virtual configuration," in Proc. Int. Symp. Autom. Robot. Constr., ISARC, vol. 35, pp. 1-8, 2018.

[21] N. A. Kumar and P. Hur, "A handheld gyroscopic device for haptics and hand rehabilitation," IEEE Trans. Haptics, vol. 15, no. 1, pp. 109-114, Jan. 2022.

[22] L. Yin, F. Wang, S. Han, Y. Li, H. Sun, Q. Lu, C. Yang, and Q. Wang, "Application of drive circuit based on L298N in direct current motor speed control system," in Proc. Adv. Laser Manuf. Technol., vol. 10153, pp. 163-169, Oct. 2016.

[23] S. A. Sawant, "IOT based control DC motor," Unpublished report.

[24] R. Gambhir and A. K. Jha, "Brushless DC motor: Construction and applications," Int. J. Eng. Sci., vol. 2, no. 5, pp. 72-77, 2013.

[25] Y. A. Badamasi, "The working principle of an Arduino," in Proc. 11th Int. Conf. Electron., Comput., Computat., ICECCO, pp. 1-4, Sep. 2014.

[26] A. S. Ismailov and Z. B. Jo'Rayev, "Study of arduino microcontroller board," Sci. Educ., vol. 3, no. 3, pp. 172-179, Mar. 2022.

[27] A. A. Galadima, "Arduino as a learning tool," in Proc. 11th Int. Conf. Electron., Comput., Computat., ICECCO, pp. 1-4, Sep. 2014.

[28] S. F. Perdana, "AC 220V digital thermostat based drying oven XH-W3001 to improve temperature accuracy in the drying process of black betel leaves (Piper betle var nigra) at PT. FBION Karanganyar," in Proc. Int. Conf. Early Child. Educ. Multiperspectives, pp. 395-406, Aug. 2023.

[29] T. Amosun and W. O. Adedeji, "Design of a PLC based temperature controlled system," REM J. Rekayasa Energi Manufaktur, vol. 8, no. 2, pp. 93-100, Nov. 2023.

[30] S. Winder, Power supplies for LED driving, Newnes, Dec. 2016.

[31] Y. M. Irwan, W. Z. Leow, M. Irwanto, M. Fareq, S. I. Hassan, I. Safwati, and A. R. Amelia, "Comparison of solar panel cooling system by using DC brushless fan and DC water," in Proc. J. Phys. Conf. Ser., vol. 622, no. 1, pp. 012001, May 2015.

Vijay Mane born on June 1, 1978, in Herwad Village, Kolhapur, Maharashtra, he is a distinguished academician and researcher in Electronics Engineering. He holds a Ph.D. from Savitribai Phule Pune University and is currently an Associate Professor at Vishwakarma Institute of Technology, Pune. With over 20 years of teaching experience, he has authored more than 50 papers in prestigious national and international journals and conferences. His research interests include Biomedical Engineering, Cybersecurity, and IoT, demonstrating his interdisciplinary expertise. His commitment to academic excellence and dedication to mentoring students highlight his invaluable contributions to advancing knowledge in Electronics Engineering.
vijay.mane@vit.edu

Harshal A. Durge was born on September 4th, 2002, in Nagpur, Maharashtra, India, He is currently pursuing a BTech degree in Electronics and Telecommunication at Vishwakarma Institute of Technology, Pune. His academic focus spans automation, electronics and IoT. His research interests are centered around advancing VLSI design, exploring applications in signal processing, developing automation technologies, and innovating within the IoT domain. His contributions have led to the publication of 6 Indian patents, showcasing his dedication to technological innovation and problem-solving. This pursuit underscores his commitment to shaping future advancements in electronic engineering and technology.
harshal.durge21@vit.edu